AIAA JOURNAL
Vol. 43, No. 2, February 2005

Reduced-Order Model for Efficient Simulation of Synthetic Jet Actuators

N. K. Yamaleev*
North Carolina A&T State University, Greensboro, North Carolina 27411
M. H. Carpenter†
NASA Langley Research Center, Hampton, Virginia 23681
and
Frederick Ferguson‡
North Carolina A&T State University, Greensboro, North Carolina 27411

A new reduced-order model of multidimensional synthetic jet actuators that combines the accuracy and conservation properties of full numerical simulation methods with the efficiency of simplified zero-order models is proposed. The multidimensional actuator is simulated by the solution of the time-dependent compressible quasi-one-dimensional Euler equations, whereas the diaphragm is modeled as a moving boundary. The governing equations are approximated with a fourth-order finite difference scheme on a moving mesh, such that one of the mesh boundaries coincides with the diaphragm. The reduced-order model of the actuator has several advantages. In contrast to the zero-dimensional models, this approach provides conservation of mass, momentum, and energy. Furthermore, the new method is computationally much more efficient than the two-dimensional Navier–Stokes simulation of the actuator cavity flow, while providing practically the same accuracy in the exterior flowfield. The most distinctive feature of the present model is its ability to predict the resonance characteristics of synthetic jet actuators; this is not practical when the three-dimensional models are used because of the computational cost involved. Numerical results demonstrating the accuracy of the new reduced-order model and its limitations are presented.

I. Introduction

INTEREST in active flow control for drag or noise reduction, flow vectoring, mixing enhancement, and separation control stimulated the recent development of innovative synthetic jet actuators that create localized disturbances in a flowfield. Synthetic jets are generated by a dynamic fluid actuator consisting of a cavity enclosed on one side by a moving diaphragm driven into transverse oscillations and on the other side by a rigid wall with a small orifice or slot, as shown in Fig. 1. The distinctive feature of these actuators is that they have jetlike characteristics without the need for mass injection. Although there is no net mass injection into the overall system over each cycle of operation, the momentum transfer into the exterior flow is nonzero. These features enable synthetic jets to effect significant global modifications in the exterior flowfield on scales that are one to two orders of magnitude larger than the characteristic length scale of the jets themselves.[1]

Accurate details of the general performance of fluid actuators is desirable over a range of flow conditions, within some predetermined error tolerance. Designers typically model actuators with different levels of fidelity depending on the acceptable level of error in each circumstance. Crude properties of the actuator, for example, peak mass rate and frequency, may be sufficient for some designs, whereas detailed information is needed for other applications, for example, multiple actuator interactions.

This work attempts to address two primary objectives. The first objective is to develop a systematic methodology for the approximation of realistic three-dimensional fluid actuators by the use of quasi-one-dimensional reduced-order models. Near full fidelity can be achieved with this approach at a fraction of the cost of full simulation and only a modest increase in cost relative to most actuator models used today. Specific considerations include 1) a general statement on which model geometries are amenable to the quasi-one-dimensional approximation, 2) regions of actuators that are inherently multidimensional and are not candidates for reduced-order modeling, and 3) the geometric features within actuators that contribute little to the fidelity of the actuator solution. The second objective, which is a direct consequence of the first, is to determine the approximate magnitude of errors committed by actuator model approximations of various fidelities. This objective attempts to identify which model (ranging from simple orifice exit boundary conditions to full numerical simulations of the actuator) is appropriate for a given error tolerance.

The numerical simulation and optimization of synthetic jet actuators has received considerable attention.[2–14] The exact nature of any actuator can be determined (in principle) by the simulation of the precise three-dimensional geometry, including all aspects of diaphragm movement and deformation. The separation of temporal and spatial scales and moving boundaries in the problem makes full computational simulation of these unsteady flows impractical. A wide range of various fidelity simplified models has been developed. The assumption of various characteristics of the actuator can significantly reduce the simulation cost. The extreme opposite full simulation is characterized by the imposition of experimental data at the actuator orifice. If reliable experimental data are available, then this approach is desirable. All general actuator models, however, fall somewhere between these two extremes and attempt to trade fidelity for cost in some measure. A brief summary of the popular methods is now presented.

One class of models attempts to impose simplified boundary conditions at the orifice exit, by directly prescribing the harmonic motion generated by the actuator. In the work of Kral et al.[2] and Donovan et al.,[3] the flow within the cavity is not calculated, and the perturbation to the flowfield is introduced through the wall-normal component of velocity at the orifice exit

$$v(x, 0, t) = V_A(x)\sin(\omega t), \qquad u(x, 0, t) = 0 \tag{1}$$

Received 19 December 2003; revision received 24 June 2004; accepted for publication 23 September 2004.

*Associate Professor, Department of Mathematics; nkyamale@ncat.edu. Member AIAA.
†Senior Research Scientist, Computational Modeling and Simulation Branch, Mail Stop 128.
‡Associate Professor, Department of Mechanical Engineering.

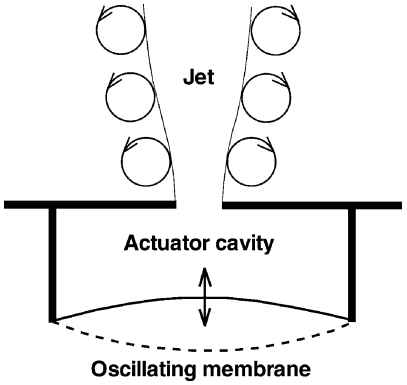

Fig. 1 Synthetic jet actuator.

where x and y are the flow streamwise and cross-stream directions, respectively. Different spatial profiles of $V_A(x)$ over the orifice have been considered. Numerical experiments[2,3] (within the scope of their model) indicate that a "top-hat" distribution most closely matches the experimental data. A modified boundary condition on the pressure at the orifice is introduced through a consideration of the normal momentum equation. When time-harmonic velocity perturbations are taken into account, this condition, obtained under the assumption that the flow is incompressible, becomes

$$\frac{\partial p}{\partial y} = -\rho V_A(x)\omega\cos(\omega t) \tag{2}$$

The numerical simulations that use the boundary conditions given by Eqs. (1) and (2) show good qualitative agreement with the experiments in Refs. 1, 15, and 16. A similar approach modeling the actuator as a blowing/suction type boundary condition that can be fully specified in advance of the calculation is used in Refs. 4–7.

An alternative technique for modeling synthetic jet actuators is proposed by Carpenter et al.[8] This actuator model is based on the classic thin-plate theory for the diaphragm dynamics. The flow through the orifice is modeled with the unsteady pipe-flow theory. This approach is based on the assumption that streamlines in the orifice exit are parallel to its axis, which is an adequate approximation if the length-to-diameter ratio is much larger than unity. The governing equation for the orifice flow is

$$\rho\frac{\partial v}{\partial t} + \frac{\rho v|v|}{2l} = -\frac{\partial p}{\partial y} + \mu r\frac{\partial}{\partial r}\left(\frac{1}{r}\frac{\partial v}{\partial r}\right) \tag{3}$$

where y and r are the axial and radial coordinates, respectively; v is the axial velocity; l is the orifice length; and ρ is taken to be the instantaneous mean of the cavity and external densities. The inertial term $\rho v v_y$ is modeled approximately by the second term on the left-hand side of Eq. (3). The dynamics of the air in the cavity is ignored, and the pressure there is calculated by means of the perfect gas law. The cavity and the external boundary-layer flowfields are linked by requiring continuity of velocity and pressure at the orifice exit. In Ref. 8, only the blowing phase of the actuator dynamics is studied.

Another zero-dimensional model based on a system of ordinary differential equations that describes a resonant fluid actuator that creates an unsteady synthetic jet through compression of fluid in a cavity is developed in Ref. 9. If the flow is isothermal and combines structural and fluid effects, a set of five coupled nonlinear first-order ordinary differential equations, including the membrane position and velocity, the fluid density and pressure, and the jet velocity, is derived. This zero-dimensional model is compared with experimental data and successfully predicts trends in the actuator behavior.

A similar reduced-order simulation of a piezoelectric-driven synthetic jet actuator with a lumped element model is performed in Ref. 10. In lumped element modeling, the individual components of the actuator are modeled as elements of an electrical circuit by the use of conjugate power variables. The linear composite plate theory is used to calculate the net volume velocity of the diaphragm and the distributed vertical velocity. The acoustic mass and resistance in the actuator neck are obtained with the incompressible fully developed laminar pipe flow theory. As a result, the lumped element model neglects the compressibility effects inside the actuator neck. The model is applied to two prototypical synthetic jets and provides fair agreement with the measured peak jet velocity. One of the conclusions of this study is that better models are needed for the unsteady flow in the orifice, including that of entrance and exit effects.

A second class of methods is based on a direct numerical simulation of the entire problem, including the flow inside the actuator. Rizzetta et al.[11] solve the unsteady compressible Navier–Stokes equations in the external region, the cavity itself, and the throat of the actuator on separate grids that are linked with each other through a Chimera methodology. The membrane motion is simulated by variation of the position of appropriate boundary points. As follows from the numerical calculations presented in Ref. 11, the internal cavity flow becomes periodic after several cycles of diaphragm oscillation. Therefore, the velocity profile across the jet exit at each time step was recorded and was used as a boundary condition in subsequent runs involving the external domain only. For computations that consider only the upper exterior domain, the transverse and spanwise velocity components (orthogonal to jet axis) are set to zero, and the inviscid normal momentum equation

$$\frac{\partial p}{\partial y} = -\rho\left(\frac{\partial v}{\partial t} + v\frac{\partial v}{\partial y}\right) \tag{4}$$

is used to establish the pressure. The density at the orifice exit is extrapolated from the interior solution. This approach provides a more accurate description of the flow details at the orifice than the simplified boundary conditions (1) and (2). Similar direct numerical simulation of the external and cavity flows is performed by Joslin et al.[12] and shows good agreement with experimental results.

Another approach that simulates the diaphragm as a moving boundary is used in Ref. 13. This technique simulates the entire actuator geometry, including the oscillating diaphragm, on a stationary Cartesian mesh. As the diaphragm moves over the underlying Cartesian mesh, the discretization in the cell cut by the solid boundary is modified to account for the presence of the diaphragm. Thus, the grid does not need to conform to the moving boundary, which simplifies the gridding of the deforming domain. This approach is applied to study the vortex dynamics, velocity profiles, and other dynamic characteristics of the incompressible low-Reynolds-number synthetic jet flow.

To avoid the integration of the Navier–Stokes equations on a moving grid, an alternative technique is used by Lee and Goldstein.[14] Their method imposes a localized body force along desired points in the computational mesh to bring the fluid there to a specified velocity so that the force has the same effect as a solid boundary. The desired velocity is incorporated in an iterative feedback loop to determine the appropriate force. For a moving boundary with velocity $V_A(x,t)$, an expression for the body force is given by

$$F(x,t) = \alpha\int_0^t (v - V_A)\,\mathrm{d}t' + \beta(v - V_A) \tag{5}$$

where v is the fluid velocity and α and β are user-defined constants that are negative and can be treated as the gain and damping of the force field. This approach simulates the moving diaphragm without the use of a time-dependent coordinate transformation.

Although the methods just mentioned have successfully been used for modeling synthetic jet actuators, several issues persist. The principle difficulty inherent in the zero-dimensional models based on Eqs. (1–4) is their inability to predict accurate pressure levels in the actuator. This is extremely apparent in the suction phase of the cycle, where pressure is the variable that determines the influx of mass. Imposition of the incorrect pressure during this phase will lead to erroneous results. The primary reason zero-dimensional models

drift away from the correct solution is that they do not conserve mass, momentum, or energy through the actuator orifice. Because these methods use the normal momentum equation to calculate the pressure, whereas the other quantities are extrapolated or prescribed analytically, these boundary conditions do not satisfy the governing equations at the boundary and, therefore, do not provide conservation properties. The zero-dimensional boundary conditions lack a mechanism to account for changes in the pressure field caused by the interaction of the external boundary layer and the actuator. Furthermore, as shown in Ref. 14, the real streamwise velocity profile and the velocity component in the crossflow direction are far from the analytical expressions of Eq. (1).

The main problem associated with the full simulation methods is computational cost. The numerical calculation of the cavity flow requires significant computational resources, sometime comparable with that needed to resolve the exterior flow. For geometries fitted with multiple actuators, grid requirements for the actuators could considerably exceed those of the exterior flow and would contribute extensively to the computational cost. The large range of temporal scales from 10^{-6} to 10^{-3} s, that is associated with the acoustic scale and the period of diaphragm oscillations makes this problem even more complicated. Another consideration is the actuator Mach number, which varies from $\mathcal{O}(10^{-3})$ (near the diaphragm) to $\mathcal{O}(1)$ (in the exterior flowfield). This variation of the flow parameters from the fully incompressible to fully compressible regimes imposes severe requirements on a numerical method and increases the algorithm complexity.

As follows from the literature overview presented, the research in the area of active flow control is of empirical nature, mainly due to the computational cost involved and lack of confidence in computational methods for such complex time-dependent flows. To overcome these problems, a new methodology that combines the accuracy and conservation properties of the full simulation methods with the efficiency of the techniques based on simplified boundary conditions is proposed. In contrast to the methods found in the literature, the new approach uses a reduced-order model to approximate the two-dimensional or three-dimensional synthetic jet actuators. If the multidimensional and viscous effects inside the actuator cavity away from the orifice exit can be neglected, the multidimensional actuator can be simulated by the solution of the time-dependent one-dimensional Euler equations similar to those used for the quasi-one-dimensional nozzle problem. The quasi-one-dimensional governing equations are written in a time-dependent coordinate frame, and the diaphragm is modeled as a moving boundary. The low-dimensional actuator model has several advantages. First, in contrast to the zero-dimensional models, this approach provides conservation of not only mass, but also momentum and energy. Second, the new method is much more efficient in terms of computational time compared with the full two-dimensional or three-dimensional numerical simulation techniques. Third, the reduced-order model retains some multidimensional features of the realistic actuator; these features are governed by the frequency and deflection of the diaphragm and the area variation and length of the quasi-one-dimensional nozzle. Therefore, the proposed reduced-order model can be used for quantitative study of the resonance characteristics of the actuator.

The paper is organized as follows. Section II describes the governing equations and boundary conditions. Section III presents the the new reduced-order model of synthetic jet actuators. A fourth-order finite difference method used to solve both the interior and exterior flows is given in Sec. IV. Section V presents the numerical results and addresses accuracy, advantages, and limitations of the new model, as well as its ability to predict the resonance characteristics of synthetic jet actuators. In Sec. VI, the questions that will be addressed in the future are discussed. Conclusions are given in Sec. VII.

II. Governing Equations and Boundary Conditions

The time-dependent two-dimensional Navier–Stokes equations are used to describe the unsteady compressible flow generated by a synthetic jet actuator. The governing equations in curvilinear coordinates (ξ, η) can be written in conservation law form as

$$\frac{\partial \hat{\boldsymbol{U}}}{\partial \tau} + \frac{\partial (\hat{\boldsymbol{F}} - \hat{\boldsymbol{F}}_v)}{\partial \xi} + \frac{\partial (\hat{\boldsymbol{G}} - \hat{\boldsymbol{G}}_v)}{\partial \eta} = 0 \tag{6}$$

where the vector of conservative variables and the inviscid and viscous fluxes are given by

$$\hat{\boldsymbol{U}} = \frac{1}{J}\boldsymbol{U}, \qquad \hat{\boldsymbol{F}} = \frac{1}{J}(\xi_x \boldsymbol{F} + \xi_y \boldsymbol{G}), \qquad \hat{\boldsymbol{G}} = \frac{1}{J}(\eta_x \boldsymbol{F} + \eta_y \boldsymbol{G})$$

$$\boldsymbol{U} = \begin{bmatrix} \rho \\ \rho u \\ \rho v \\ \rho e \end{bmatrix}, \qquad \boldsymbol{F} = \begin{bmatrix} \rho u \\ \rho u^2 + p \\ \rho v u \\ u(\rho e + p) \end{bmatrix}, \qquad \boldsymbol{G} = \begin{bmatrix} \rho v \\ \rho v u \\ \rho v^2 + p \\ v(\rho e + p) \end{bmatrix}$$

$$\hat{\boldsymbol{F}}_v = \frac{1}{J}\begin{bmatrix} 0 \\ \xi_{x_i}\tau_{i1} \\ \xi_{x_i}\tau_{i2} \\ \xi_{x_i}(u_j\tau_{ij} - q_i) \end{bmatrix}, \qquad \boldsymbol{G}_v = \frac{1}{J}\begin{bmatrix} 0 \\ \eta_{x_i}\tau_{i1} \\ \eta_{x_i}\tau_{i2} \\ \eta_{x_i}(u_j\tau_{ij} - q_i) \end{bmatrix}$$

$$\tau_{ij} = \frac{\mu}{Re_\infty}\left(\frac{\partial \xi_k}{\partial x_j}\frac{\partial u_i}{\partial \xi_k} + \frac{\partial \xi_k}{\partial x_i}\frac{\partial u_j}{\partial \xi_k} - \frac{2}{3}\delta_{ij}\frac{\partial \xi_l}{\partial x_k}\frac{\partial u_k}{\partial \xi_l}\right)$$

$$q_i = -\frac{\mu}{Re_\infty Pr(\gamma - 1)M_\infty^2}\frac{\partial \xi_j}{\partial x_i}\frac{\partial T}{\partial \xi_j}$$

$$\begin{bmatrix} u_1 \\ u_2 \end{bmatrix} = \begin{bmatrix} u \\ v \end{bmatrix}, \qquad \begin{bmatrix} x_1 \\ x_2 \end{bmatrix} = \begin{bmatrix} x \\ y \end{bmatrix}, \qquad \begin{bmatrix} \xi_1 \\ \xi_2 \end{bmatrix} = \begin{bmatrix} \xi \\ \eta \end{bmatrix}$$

The variables ρ, u, v, p, and e are the density, Cartesian velocity components, pressure, and total specific energy, respectively. All of the length scales and dependent variables have been nondimensionalized by the slot width d and the corresponding reference values, respectively, except for p, which has been normalized by $\rho_\infty u_\infty^2$, where ρ_∞ and u_∞ are the freestream density and velocity, respectively. The Sutherland law for the viscosity coefficient μ and the equation of state for a perfect gas

$$p = (\gamma - 1)\rho\left[e - \tfrac{1}{2}(u^2 + v^2)\right]$$

are used to close Eq. (6). The ratio of specific heats γ is assumed to be 1.4. Note that the ξ and η coordinates in Eq. (6) do not depend on time, that is, the two-dimensional Navier–Stokes equations are solved on a stationary grid.

The governing equations are closed with the following boundary conditions. A no-slip boundary condition for the velocity vector and a constant wall temperature are imposed on the wall surface

$$u|_{\text{wall}} = v|_{\text{wall}} = 0, \qquad T|_{\text{wall}} = T_\infty \tag{7}$$

The Blasius profile is used to set the solution vector at the inflow. At the subsonic outflow boundary, a boundary condition for the pressure is imposed weakly. Characteristic conditions are applied at the upper boundary so that the vortex structures can leave the computational domain without producing perceptible spurious reflections. The unsteady flow inside the actuator cavity, generated by harmonic motion of the diaphragm, is modeled by using a new reduced-order model described in the next section.

III. Reduced-Order Model of Synthetic Jet Actuators

A gap exists between the zero-dimensional models and the full two-dimensional/three-dimensional models of a synthetic jet actuator. To combine the accuracy and conservation properties of the full numerical simulation methods with the efficiency of the simplified blowing/suction type boundary conditions, a new reduced-order model of a multidimensional synthetic jet actuator is proposed. In contrast to the methods available in the literature, the new approach uses a reduced-order model to approximate a two-dimensional or

three-dimensional actuator. The multidimensional actuator is simulated by the solution of the time-dependent one-dimensional Euler equations similar to those used for the quasi-one-dimensional nozzle problem. The time-dependent quasi-one-dimensional Euler equations can be written in the following conservation law form:

$$\frac{\partial \boldsymbol{U}}{\partial t} + \frac{\partial \boldsymbol{E}}{\partial y} + \boldsymbol{H} = 0 \tag{8}$$

$$\boldsymbol{U} = A\begin{bmatrix}\rho\\ \rho v\\ \rho e\end{bmatrix}, \qquad \boldsymbol{E} = A\begin{bmatrix}\rho v\\ \rho v^2 + p\\ v(\rho e + p)\end{bmatrix}, \qquad \boldsymbol{H} = -\begin{bmatrix}0\\ p\dfrac{\partial A}{\partial y}\\ 0\end{bmatrix}$$

where A is the cross-sectional area of the quasi-one-dimensional actuator. It is assumed that A is a continuously differentiable function that is independent of time, that is, $A = A(y)$.

To simulate the diaphragm dynamics, a time-dependent one-to-one coordinate transformation

$$\tau = t, \qquad \zeta = \zeta(t, y) \tag{9}$$

is employed to map a physical domain with the moving boundary onto a unit interval. Note that the ζ coordinate depends on time, and, therefore, a moving mesh technique is applied to solve the quasi-one-dimensional Euler equations. Because the frequency of diaphragm oscillations ω is a given quantity, the moving mesh can be generated analytically:

$$y(\zeta, \tau) = (1 - \zeta)\{L + a[1 - \cos(\omega\tau)]\} \tag{10}$$

where y and ζ are physical and computational coordinates, respectively; a and ω are the amplitude and frequency of the quasi-one-dimensional piston; and $L + a$ is a mean depth of the quasi-one-dimensional synthetic jet actuator. The amplitude a is chosen such that the mass rate at the quasi-one-dimensional piston is precisely equal to that of the realistic multidimensional actuator diaphragm. Note that the new reduced-order model can be used if the diaphragm dynamics is measured experimentally or defined by a more general function than $a[1 - \cos(\omega\tau)]$, for example, when amplitude modulation is employed.

The quasi-one-dimensional Euler equations in the time-dependent coordinate frame can be rewritten in conservation law form as

$$\frac{\partial \bar{\boldsymbol{U}}}{\partial \tau} + \frac{\partial \bar{\boldsymbol{E}}}{\partial \zeta} + \bar{\boldsymbol{H}} = 0 \tag{11}$$

where

$$\bar{\boldsymbol{U}} = \boldsymbol{U}/J, \qquad \bar{\boldsymbol{E}} = (1/J)(\zeta_t \boldsymbol{U} + \zeta_y \boldsymbol{E}), \qquad \bar{\boldsymbol{H}} = \boldsymbol{H}/J, \qquad J = 1/y_\zeta$$

Diaphragm oscillations are forced by variation of the position of the right boundary $y(0, \tau)$, where the impermeable wall boundary condition is imposed. Because the deforming mesh equation (10) is given analytically, the diaphragm velocity can be calculated by differentiation of Eq. (10) with respect to time to give

$$v(0, \tau) = a\omega \sin(\omega\tau) \tag{12}$$

Note that the region near the jet exit requires special consideration. As shown in Ref. 11, the full numerical simulation of the actuator orifice region is crucial for accurate prediction of the interaction between the synthetic jet and the external boundary layer. This region is characterized by strong flow separation that cannot be described by the quasi-one-dimensional Euler equations. To overcome this problem, the quasi-one-dimensional actuator model is used only to simulate the flow inside the actuator cavity, whereas the small region near the actuator orifice is modeled by solving the two-dimensional unsteady Navier–Stokes equations. The new reduced-order model is shown schematically in Fig. 2. The region where the quasi-one-dimensional Euler equations are used is bounded by the dashed line, whereas in the rest of the domain the two-dimensional Navier–Stokes equations are applied. This approach allows us to accurately predict the interaction of the synthetic jet with the external boundary layer and to resolve vortices generated in the vicinity of the actuator orifice while reducing the computational cost.

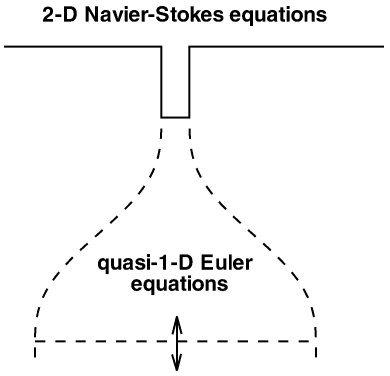

Fig. 2 Reduced-order model of a synthetic jet actuator.

The low-dimensional actuator model has several advantages. First, this approach is fully conservative and provides conservation of mass, momentum, and energy. Second, the new quasi-one-dimensional model is computationally much more efficient compared with the two-dimensional or three-dimensional numerical simulation of the cavity flow. Third, the reduced-order model retains some important multidimensional features of the realistic actuator, such as the length, diaphragm deflection, and area variation. These properties of the new model and its ability to account for the compressibility effects inherent in actuator devices make it an efficient tool for quantitative study of the actuator resonance characteristics.

The proposed reduced-order model is based on the assumption that the multidimensional and viscous effects inside the actuator cavity away from the orifice exit can be neglected. The detailed validation of this assumption for a broad range of flow parameters and actuator geometries is presented in Sec. V.

IV. Fourth-Order Numerical Method

A fourth-order upwind-biased linear finite difference scheme based on the local Lax–Friedrichs flux splitting is used to discretize both the two-dimensional Navier–Stokes equations (6) and the quasi-one-dimensional Euler equations (11). This scheme can be written in a semidiscrete form as

$$\frac{\mathrm{d}\hat{\boldsymbol{U}}}{\mathrm{d}\tau} + \frac{1}{2}\left(D^-_{4\xi}\hat{\boldsymbol{F}}^+ + D^+_{4\xi}\hat{\boldsymbol{F}}^- + D^-_{4\eta}\hat{\boldsymbol{G}}^+ + D^+_{4\eta}\hat{\boldsymbol{G}}^-\right) = D^c_{4\xi}\hat{\boldsymbol{F}}_v + D^c_{4\eta}\hat{\boldsymbol{G}}_v \tag{13}$$

where $D^\pm_{4\xi}$, $D^c_{4\xi}$ and $D^\pm_{4\eta}$, $D^c_{4\eta}$ are linear fourth-order finite difference operators in ξ and η, respectively. The Lax–Friedrichs fluxes are given by

$$\hat{\boldsymbol{F}}^\pm = \hat{\boldsymbol{F}} \pm \left|\lambda^{\max}_\xi\right|\hat{\boldsymbol{U}}, \qquad \hat{\boldsymbol{G}}^\pm = \hat{\boldsymbol{G}} \pm \left|\lambda^{\max}_\eta\right|\hat{\boldsymbol{U}} \tag{14}$$

where $|\lambda^{\max}_\xi|$ and $|\lambda^{\max}_\eta|$ are the local maximum values of the contravariant eigenvalues $|\hat{u}| + \hat{c}$ and $|\hat{v}| + \hat{c}$, accordingly.

In the present analysis, the following upwind-biased fourth-order spatial operators $D^\pm_4$ are used to discretize the inviscid fluxes:

$$D^-_4 f_j = (1/12h)(-f_{j-3} + 6f_{j-2} - 18f_{j-1} + 10f_j + 3f_{j+1})$$
$$D^+_4 f_j = (1/12h)(-3f_{j-1} - 10f_j + 18f_{j+1} - 6f_{j+2} + f_{j+3}) \tag{15}$$

where h is a grid spacing in either ξ or η. The viscous fluxes are approximated by a fourth-order central finite difference operator given by

$$D^c_4 f_j = (1/12h)(f_{j-2} - 8f_{j-1} + 8f_{j+1} - f_{j+1}) \tag{16}$$

The third-order boundary closures used near the boundaries are the optimal stencils derived from nearest neighbor information, biased where possible in an upwind direction.

The interface, inflow, and outflow boundary conditions are imposed weakly. The weak formulation of the wall boundary condition requires too many grid points near the wall to satisfy the no-slip condition. Therefore, the no-slip boundary condition for the velocity vector is imposed in the strong sense, which considerably decreases the number of grid points in the boundary layer while preserving the overall accuracy of the numerical solution. To satisfy the conservation laws at the interface between the two-dimensional and quasi-one-dimensional domains, the two-dimensional vector of conservative variables is "one-dimensionalized" as follows:

$$\bar{\boldsymbol{U}} = \int_0^d \boldsymbol{U}(x, 0)\,\mathrm{d}x$$

The preceding vector and the solution of the quasi-one-dimensional Euler equations at the interface are then used as the left and right states of the Riemann problem that is solved approximately. The weak formulation of the interface boundary condition provides the conservation of mass, momentum, and energy and allows the ambient fluid to be entrained into the cavity and expelled via the jet.

The quasi-one-dimensional Euler and two-dimensional Navier–Stokes equations are integrated in time by the use of a five-stage, low-storage, explicit Runge–Kutta method developed in Ref. 17. When the governing equations are written as an initial value problem

$$\frac{\partial \boldsymbol{U}}{\partial t} = \mathrm{RHS}(\boldsymbol{U})$$

the low-storage explicit Runge–Kutta method is implemented as follows:

$$\boldsymbol{U}^1 = \boldsymbol{U}^n, \qquad \boldsymbol{dU}^l = a_l \boldsymbol{dU}^{l-1} + \mathrm{RHS}(\boldsymbol{U}^{l-1}), \qquad l = \overline{2,5}$$

$$\boldsymbol{U}^l = \boldsymbol{U}^{l-1} + b_l \boldsymbol{dU}^l, \qquad \boldsymbol{U}^{n+1} = \boldsymbol{U}^5$$

where a_l and b_l are functions of the standard Butcher coefficients and $\boldsymbol{U}^{n+1}$ is the fourth-order solution at time level $n+1$. The main advantage of this Runge–Kutta scheme is considerable reduction of computer memory usage because only two storage registers are required during the numerical integration.

V. Numerical Results

To evaluate accuracy and limitations of the new reduced-order model, the interaction between a synthetic jet actuator and a boundary layer near a flat plate is used as a test problem. The following atmospheric conditions are assumed for both freestream density $\rho_\infty = 0.365$ kg/m^3 and temperature $T_\infty = 217$ K. For all of the test examples considered, the freestream Mach number is chosen to be 0.5, which corresponds to a subsonic regime in the entire flowfield. For these flow parameters, the Reynolds number based on the freestream velocity and the flat-plate length varies from 2.4×10^4 to 1.2×10^5, whereas the Reynolds number based on the actuator orifice size $Re_d = \rho_\infty u_\infty \mathrm{d}/\mu_\infty$ (where ρ_∞, u_∞, and μ_∞ are the freestream density, velocity, and viscosity, respectively, and d is the slot width) varies from 2×10^2 to 10^3. Therefore, the flow in the entire domain is assumed to be laminar. Two two-dimensional actuator cavity shapes, box and nozzle-type geometries, are considered in the present analysis. It is assumed that the actuator geometries are rectangular and that all of the derivatives with respect to the third coordinate are equal to zero. For all of the nozzle-type actuators considered, the geometry profile is given by the following seventh-order polynomial:

$$A(\bar{\zeta}) = A_o + (A_o - A_d)\bar{\zeta}^4(-35 + 84\bar{\zeta} - 70\bar{\zeta}^2 + 20\bar{\zeta}^3)$$

where $\bar{\zeta} = (y - y_o)/(y_d - y_o)$ and A_d and A_o are areas of the actuator diaphragm and orifice, respectively.

Because the exact solution to this complicated time-dependent problem is not available, the accuracy of the reduced-order model is evaluated by comparison of the numerical solutions obtained with the quasi-one-dimensional model and the full two-dimensional Navier–Stokes simulation of the same actuator. To avoid the integration of the two-dimensional Navier–Stokes equations on a moving grid, the diaphragm dynamics is simulated by the use of the quasi-one-dimensional Euler equations. In other words, the two-dimensional Navier–Stokes equations are employed in the entire actuator cavity, except for a small region near the moving diaphragm that is modeled in a quasi-one-dimensional sense, as described in Sec. III. This treatment of the moving diaphragm allows us to perform full two-dimensional numerical simulations without using a time-dependent coordinate transformation. Because the region where the quasi-one-dimensional Euler equations are used is much smaller than that described by the two-dimensional Navier–Stokes equations, this combined approach accounts for the multidimensional and viscous effects inside the actuator cavity and provides high accuracy of the numerical solution.

A. Validation of Zero-Dimensional Model

Before the new reduced-order model of synthetic jet actuators is validated, a conventional zero-dimensional model is tested. To incorporate the zero-dimensional model into the high-order finite difference formulation used in the present analysis, the blowing/suction boundary conditions (1) and (4) are imposed in the weak sense. To be consistent with the zero-dimensional model, the diaphragm deflection in the quasi-one-dimensional and two-dimensional simulations is adjusted such that the peak mass rate at the orifice exit equals to that prescribed in the boundary conditions (1) and (4). In contrast to the zero-dimensional models available in the literature, in the present analysis, the blowing/suction boundary conditions are imposed inside the actuator neck rather than at the orifice exit. This implementation of the boundary conditions makes the zero-dimensional model more accurate because the viscous effects near the jet exit are taken into account. It also makes the comparison between zero-dimensional and quasi-one-dimensional models more consistent because the boundary conditions are imposed along the same line where the interface between the quasi-one-dimensional and two-dimensional models is located.

One distinctive feature of synthetic jet actuators is that the net mass injection into the overall system over each cycle of operation is zero. This characteristic feature of synthetic jet actuators is used to estimate accuracy of the zero-dimensional and quasi-one-dimensional models. A nozzle-type actuator geometry used in this study is shown in Fig. 3. Three calculations corresponding to different locations of the interface between the low-dimensional model and the full two-dimensional model are performed. The computational parameters are as follows: $Re_d = 5 \times 10^2$, $L = 20$, $\omega = 0.1257$, and $a = 0.2387$. The total mass injection over a period of diaphragm oscillation, obtained with the zero-dimensional and quasi-one-dimensional models, is presented in Table 1. As follows from these results, the quasi-one-dimensional model is one order of magnitude more accurate than its zero-dimensional counterpart. This result is not surprising because the blowing/suction boundary conditions do not satisfy the conservation laws, whereas the new reduced-order model is based on the conservation laws equations.

To demonstrate the superiority of the new reduced-order model over the transpiration boundary conditions (1) and (4), time histories of the wall pressure integrals obtained with the zero-dimensional,

Table 1 Total mass injection over a period of diaphragm oscillation

Interface location (distance from surface)	Zero-dimensional model[a]	Quasi-one-dimensional model[a]
$2d$	0.729	0.0622
$5d$	1.326	0.0113
$10d$	2.046	0.0902

[a]Mass $\times 10^2$.

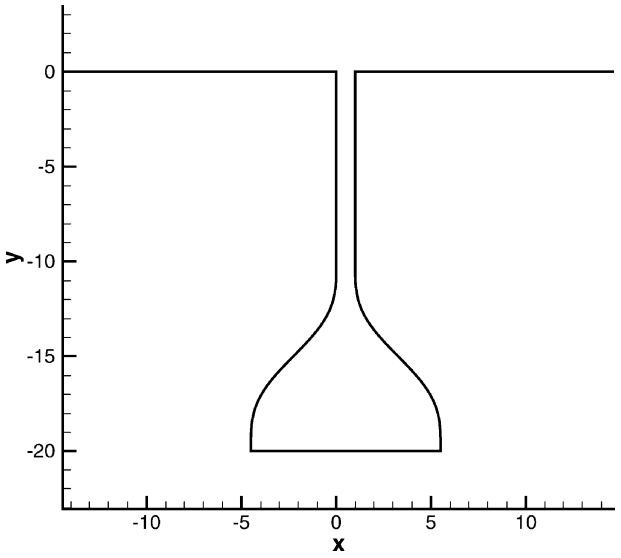

Fig. 3 Two-dimensional actuator geometry used for validation of the zero-dimensional model and the study of the sensitivity of the quasi-one-dimensional model to interface location.

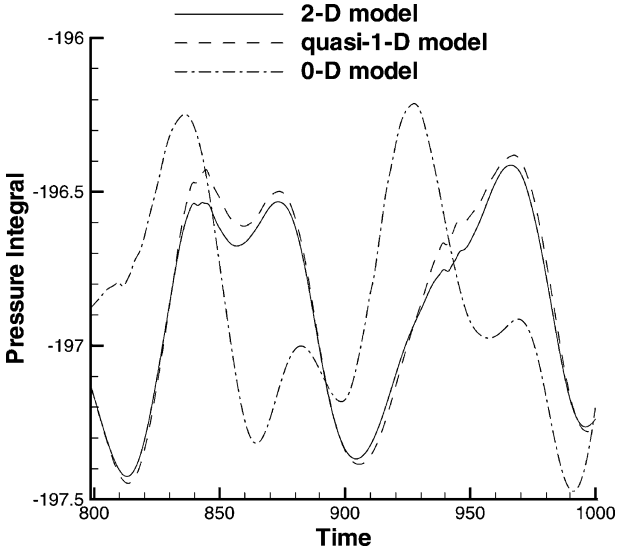

Fig. 4 Time histories of the pressure integral obtained with zero-dimensional, quasi-one-dimensional, and two-dimensional models.

quasi-one-dimensional, and two-dimensional models are compared in Fig. 4. The wall pressure integral, which can be interpreted as the lift coefficient, is defined as follows:

$$I_p = \int_1^{x_{\max}} p(x, 0)\, \mathrm{d}x \tag{17}$$

where $x = 1$ is the downstream corner of the orifice exit and $x_{\max}$ is the x coordinate of the downstream end of the flat plate. As seen in Fig. 4, the pressure integrals obtained with the quasi-one-dimensional and full two-dimensional models are in a good agreement, whereas the zero-dimensional model results are completely inaccurate. The lack of accuracy of the zero-dimensional model is due to the heuristic assumptions about the velocity profile and pressure gradient that have been made to construct the simplified boundary conditions (1) and (4).

B. Validation of the Quasi-One-Dimensional Model

To validate the new reduced-order model, the synthetic jet generated by a nozzle-type actuator with a long $10d$ neck, shown in Fig. 5, is simulated with both the quasi-one-dimensional and two-dimensional models. Note that the quasi-one-dimensional cavity

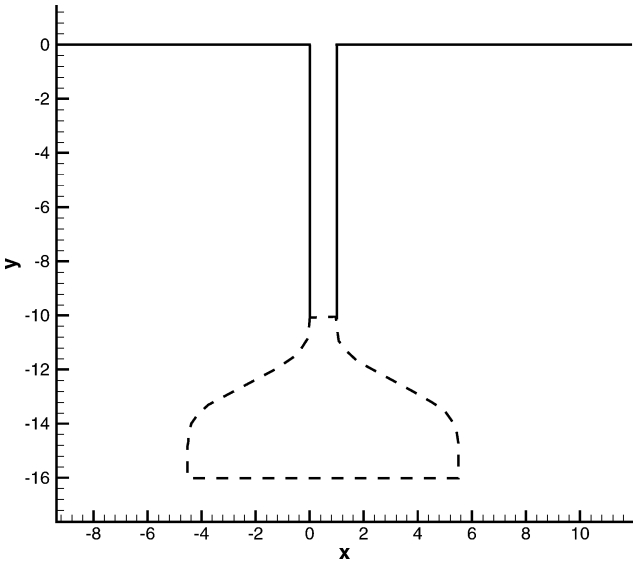

Fig. 5 Two-dimensional actuator geometry used for validation of the quasi-one-dimensional model.

geometry shown with the dashed line precisely coincides with the two-dimensional actuator geometry.

A four-block structured computational grid having 281×101 grid points in the exterior region and 81×201 points inside the actuator cavity is used in the present analysis. The grid points are clustered along the solid surfaces such that about 20 grid points are located inside the boundary layer. The Reynolds number, nondimensional diaphragm deflection, and frequency are 10^3, 0.887, and 0.0338, respectively.

Snapshots of vorticity contours obtained with both the quasi-one-dimensional and two-dimensional models at three phase angles of diaphragm oscillation ($\omega t = 0, \pi/2$, and π) are presented in Fig. 6. The quasi-one-dimensional and two-dimensional solutions at the phase angle $3\pi/2$ are practically identical and, therefore, not presented in Fig. 6. The 0 and π phase angles correspond to the maximum and minimum values of the actuator cavity volume, respectively. Although the quasi-one-dimensional model does not model the boundary layer and its separation inside the actuator cavity, the conservation properties of the new model and the detailed simulation of the flow recirculation near the slot exit provide very good accuracy compared with the full two-dimensional model.

To show how accurately the new quasi-one-dimensional actuator model predicts the synthetic jet characteristics, Fig. 7 presents the jet mass rates at the orifice exit, obtained with the reduced-order and full two-dimensional models. The maximum deviation between the quasi-one-dimensional and two-dimensional solutions is about 3–5%. This difference occurs because the quasi-one-dimensional Euler equations do not account for the viscous losses inside the actuator cavity. The results presented in Fig. 7 indicate that the multidimensional and viscous phenomena associated with the boundary layer and its separation inside the actuator cavity away from the orifice have almost no effect on either the synthetic jet characteristics or the exterior flow.

C. Sensitivity of the Quasi-One-Dimensional Model to Reynolds Number

As mentioned in Sec. III, the new reduced-order model does not account for the viscous losses that occur inside the actuator cavity. To evaluate the effect of viscosity on accuracy of the quasi-one-dimensional model of a nozzle-type actuator geometry shown in Fig. 8, three calculations at Reynolds numbers 2×10^2, 5×10^2, and 10^3 are performed. For all three calculations, the amplitude and frequency of diaphragm oscillation remain unchanged and equal to 0.4775 and 0.0628, respectively.

At $Re_d = 2 \times 10^2$, the viscous effects are predominant. As can be seen in Fig. 9, the flow is fully developed not only inside the actuator

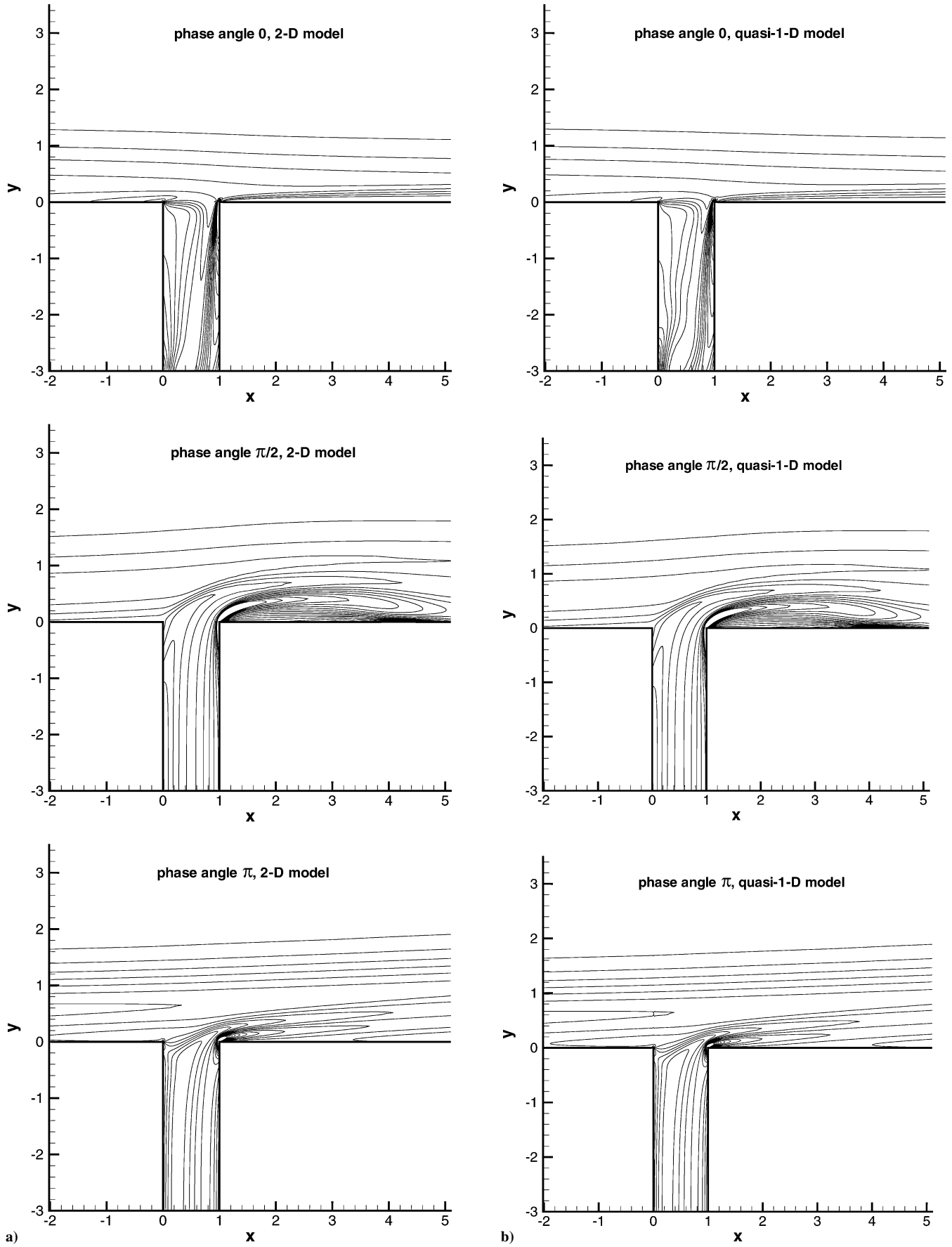

Fig. 6 Vorticity contours at phase angles 0, $\pi/2$, and π obtained with the a) two-dimensional and b) quasi-one-dimensional models.

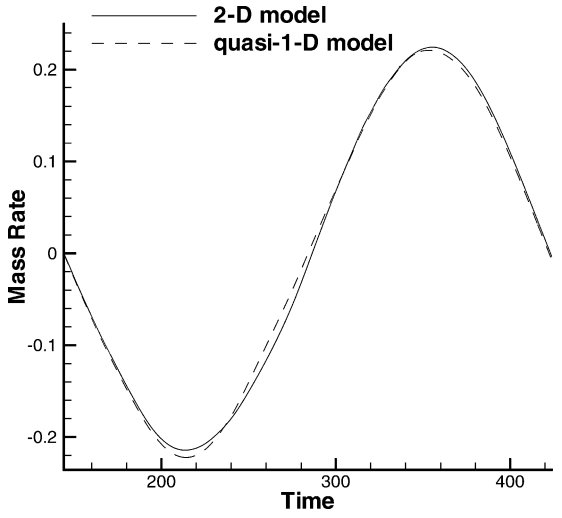

Fig. 7 Time histories of the jet mass rate at the orifice exit obtained with the quasi-one-dimensional and two-dimensional models.

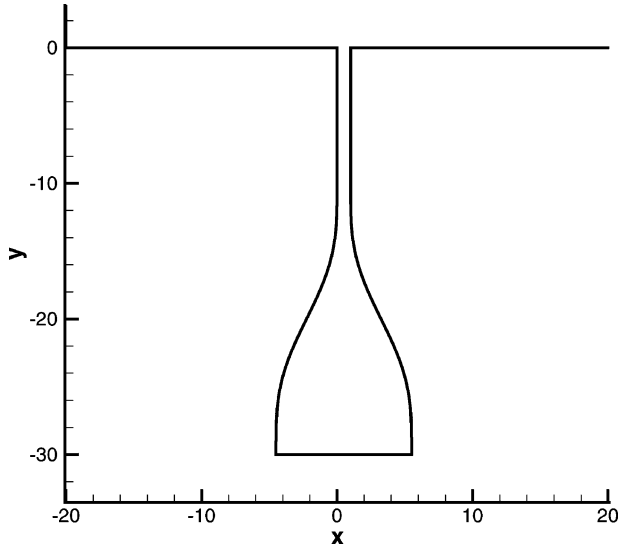

Fig. 8 Two-dimensional actuator geometry used for the study of the sensitivity of the quasi-one-dimensional model to the Reynolds number.

neck but also in the region of rapid area variation $-15 \le y \le -10$. The growth of the boundary layer restricts the mass flow through this region. In the reduced-order model, this region is simulated with the quasi-one-dimensional Euler equations that do not account for these viscous effects. As a result, the synthetic jet mass rate predicted by the quasi-one-dimensional model at $Re_d = 2 \times 10^2$ is about 20% larger than that obtained with the full two-dimensional Navier–Stokes simulation of the cavity flow, as seen in Fig. 10. As the Reynolds number increases, the viscous effects inside the actuator cavity become weaker, which leads to a better agreement between the quasi-one-dimensional and two-dimensional models. As expected, the quasi-one-dimensional model provides the highest accuracy for the largest Reynolds number considered. For $Re_d = 5 \times 10^2$ and $Re_d = 10^3$, the synthetic jet mass rates obtained with the quasi-one-dimensional and two-dimensional models during the periodic regime agree to within 5–10%. Based on the results presented in Fig. 10, we conclude that the new reduced-order model accurately predicts the synthetic jet characteristics of this geometry for $Re_d \ge 5 \times 10^2$.

D. Sensitivity of the Quasi-One-Dimensional Model to Interface Location

Another issue that requires special investigation is sensitivity of the new reduced-order model to a location of the interface

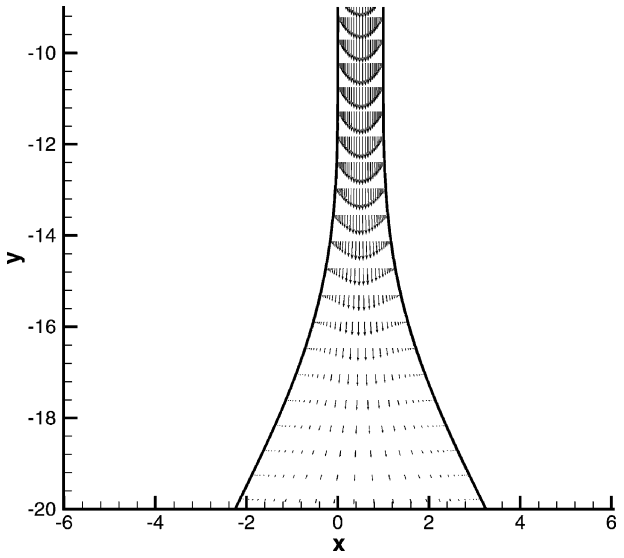

Fig. 9 Instantaneous velocity field inside the actuator cavity, obtained with the full two-dimensional model at $Re_d = 2 \times 10^2$.

between the quasi-one-dimensional Euler equations and the two-dimensional Navier–Stokes equations. As mentioned earlier, the quasi-one-dimensional model is not valid near the orifice exit where the strong boundary-layer separation occurs, which should be simulated with the full two-dimensional Navier–Stokes equations. To quantify the influence of interface location on the overall numerical solution accuracy, four calculations with the interface located $1d$, $2d$, $5d$, and $10d$ away from the orifice exit are carried out.

The Reynolds number and the cavity depth are chosen to be 5×10^2 and 20, respectively; the diaphragm deflection and frequency are equal to those used in the foregoing test problem. A two-dimensional actuator geometry used for this sensitivity analysis is shown in Fig. 3. Figure 11 shows the effect of interface location on the predicted temporal variation of the synthetic jet mass rate at the orifice exit. The closer the interface is located to the flat plate surface, the less accurate the quasi-one-dimensional model becomes. The main reason for such a behavior is the inability of the quasi-one-dimensional Euler equations to describe the flow recirculation near the jet exit. However, if the interface is located more than $2d$ away from the orifice exit, the agreement between the quasi-one-dimensional model and the two-dimensional full Navier–Stokes simulation is good. These results suggest that only the small region near the jet exit, which is comparable with the actuator slot size, should be simulated by the use of the two-dimensional Navier–Stokes equations, whereas the rest of the cavity flow can be accurately predicted by the quasi-one-dimensional Euler equations.

E. Sensitivity of Quasi-One-Dimensional Model to Actuator Geometry

The results presented so far were obtained for the nozzle-type actuators with long necks. To test the sensitivity of the new quasi-one-dimensional model to actuator geometry, a $21d \times 20d$ box actuator with a very short $1d$ neck is considered. The calculation is performed at $Re_d = 10^3$, $\omega = 0.02255$, and $a = 0.887$. In contrast to the nozzle-type profile, the box geometry has sharp corners inside the actuator cavity that cannot be accurately approximated by a smooth area variation function $A(y)$. Note that the quasi-one-dimensional Euler equations are derived under the assumption that the area $A(y)$ is a continuously differentiable function. Furthermore, these sharp corners cause the strong flow separation and generate vortices inside the actuator cavity during the expulsion and ingestion strokes. These conditions indicate that not only the actuator neck, but also a small portion of the actuator cavity near the jet exit should be simulated by the use of the two-dimensional Navier–Stokes equations. To overcome this problem and simultaneously reduce the computational cost, the quasi-one-dimensional Euler equations are used to

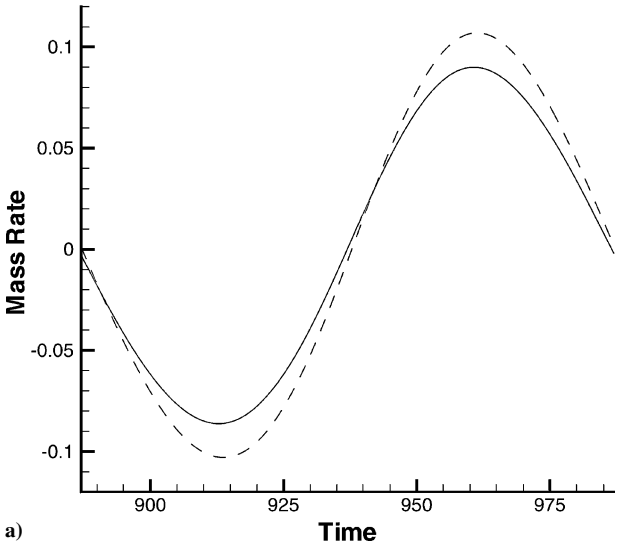

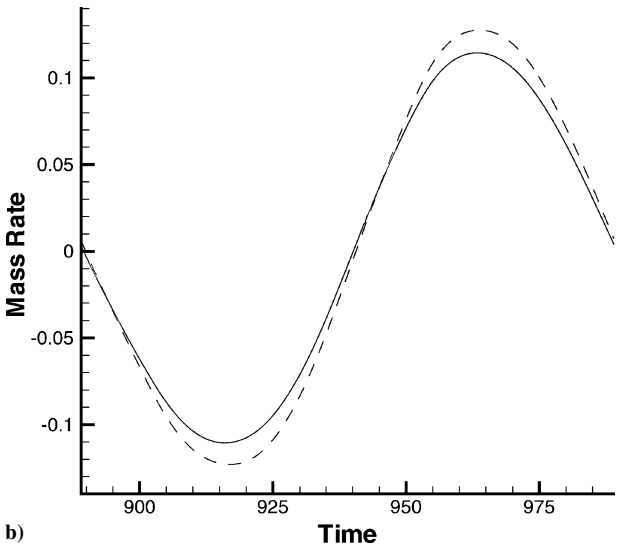

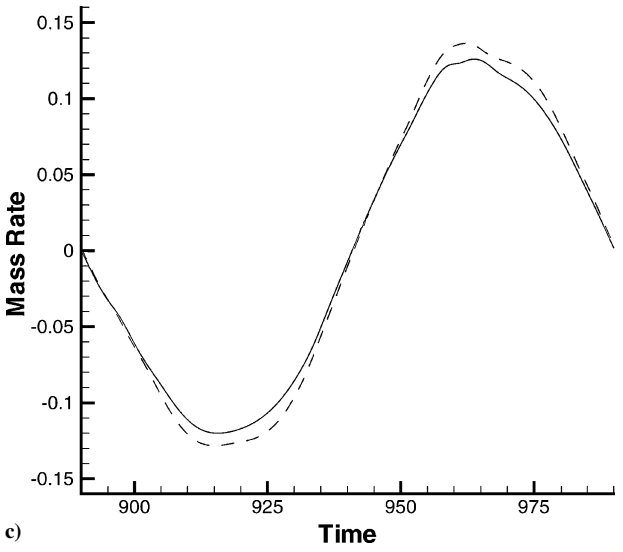

Fig. 10 Time histories of the jet mass rate obtained with ----, the quasi-one-dimensional and ——, the two-dimensional models: a) $Re_d = 2 \times 10^2$, b) $Re_d = 5 \times 10^2$, and c) $Re_d = 10^3$.

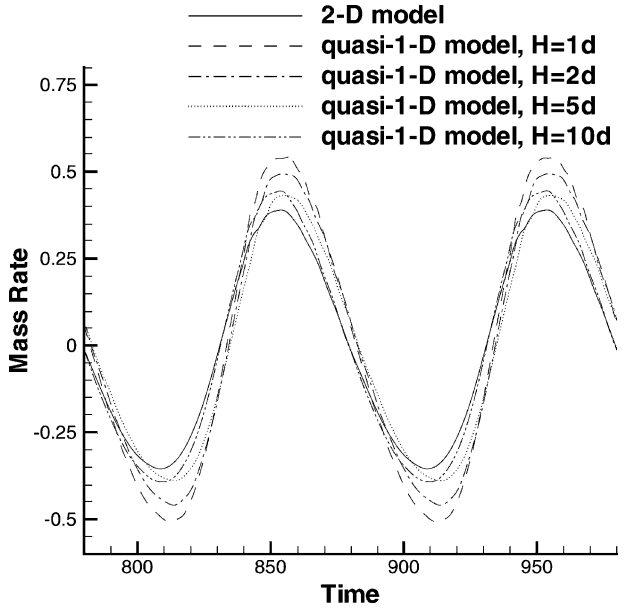

Fig. 11 Effect of the interface location on accuracy of the quasi-one-dimensional model.

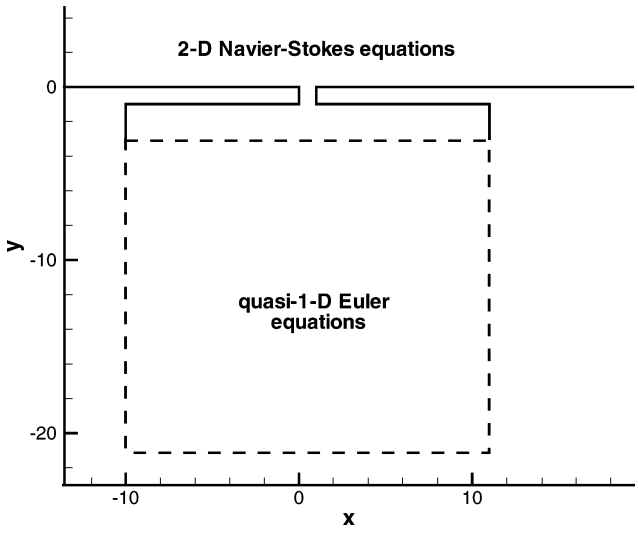

Fig. 12 Quasi-one-dimensional cavity geometry for box actuator.

solve 90% of the cavity flow; the remaining actuator flowfield near the orifice exit is described by the two-dimensional Navier–Stokes equations, as shown in Fig. 12. The actual quasi-one-dimensional cavity geometry shown with the dashed line coincides with that of the two-dimensional actuator.

To demonstrate the effect of actuator geometry on accuracy of the new reduced-order model, time histories of the mass rate at the orifice exit, as predicted by the quasi-one-dimensional model and the full two-dimensional Navier–Stokes simulation, are compared in Fig. 13. Although the quasi-one-dimensional Euler equations do not describe the complex behavior of vortex structures inside the actuator cavity, the agreement between the reduced-order model and the full two-dimensional simulation in the exterior flowfield is excellent. In contrast to the zero-dimensional models, the new quasi-one-dimensional model does not require any information about the velocity profile at the jet exit. This property of the new model is demonstrated in Fig. 14, which shows the instantaneous jet velocity profiles measured at the slot exit at four phase angles of diaphragm oscillation $\omega t = 0$, $\pi/2$, π, and $3\pi/2$. The jet velocity profiles are essentially asymmetric with a peak near the downstream edge of the orifice exit and resemble neither the top-hat

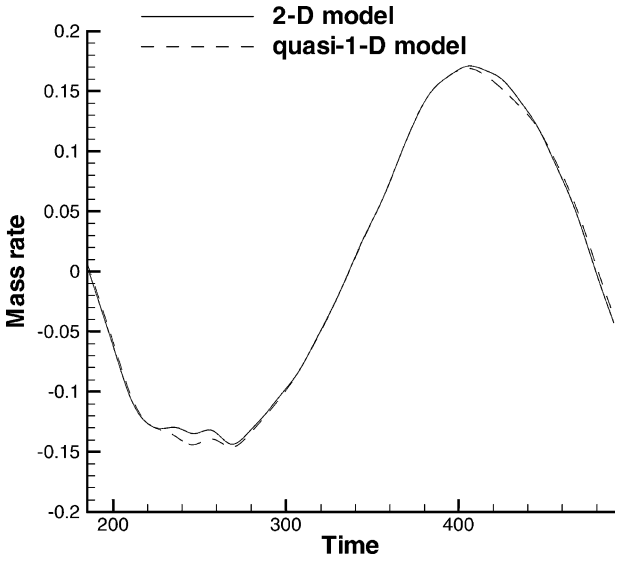

Fig. 13 Time histories of the mass rate obtained with the quasi-one-dimensional and two-dimensional models for the box actuator.

nor the sinusoidal profiles of Kral et al.[2] Although the multidimensional effects are essential near the orifice exit, the results obtained with the quasi-one-dimensional model are in a very good agreement with that of the full two-dimensional model.

All of the comparisons presented so far have been performed for the quantities at the orifice exit and in the exterior flowfield. It would also be of interest to quantify the error inside the actuator cavity committed by the quasi-one-dimensional model. However, the reduced-order model solution is essentially one-dimensional and cannot be directly compared with the two-dimensional Navier–Stokes solution inside the cavity. To compare the quasi-one-dimensional and two-dimensional solutions, the two-dimensional Navier–Stokes solution is one-dimensionalized as follows:

$$\boldsymbol{U}_{1D}(y) = \frac{1}{A(y)} \int_{x_l(y)}^{x_r(y)} \boldsymbol{U}(x, y)\, \mathrm{d}x$$

where A is the cross-sectional area of the two-dimensional actuator cavity, x_l and x_r are x coordinates of the left and right cavity boundaries, and $\boldsymbol{U}$ is the two-dimensional Navier–Stokes solution. The velocity distributions inside the cavity as predicted by the quasi-one-dimensional and two-dimensional models are compared in Fig. 15. The discrepancy between the reduced-order model and the

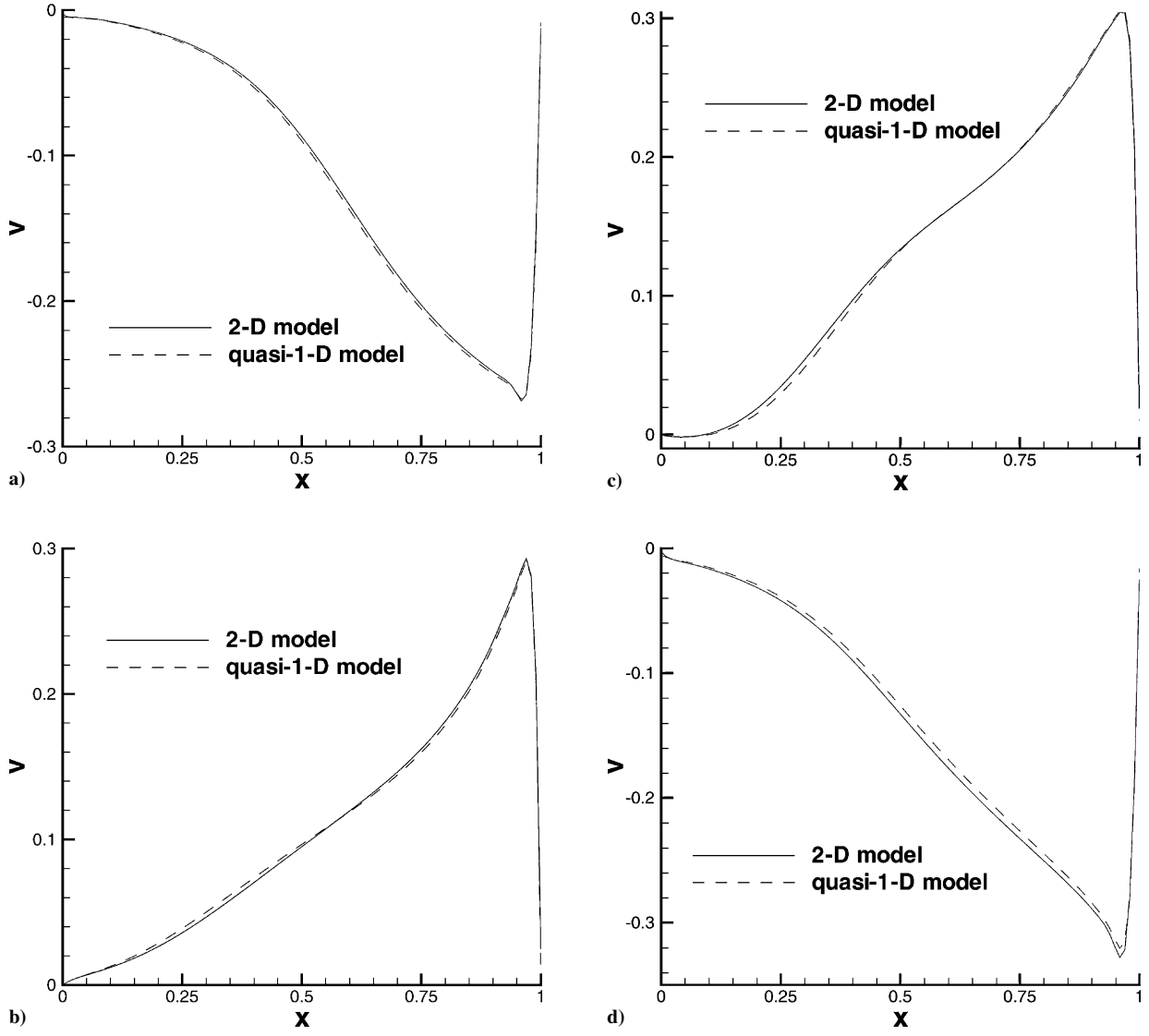

Fig. 14 Instantaneous jet velocity profiles obtained with the quasi-one-dimensional and two-dimensional models for the box actuator at phase angles a) 0, b) $\pi/2$, c) π, and d) $3\pi/2$.

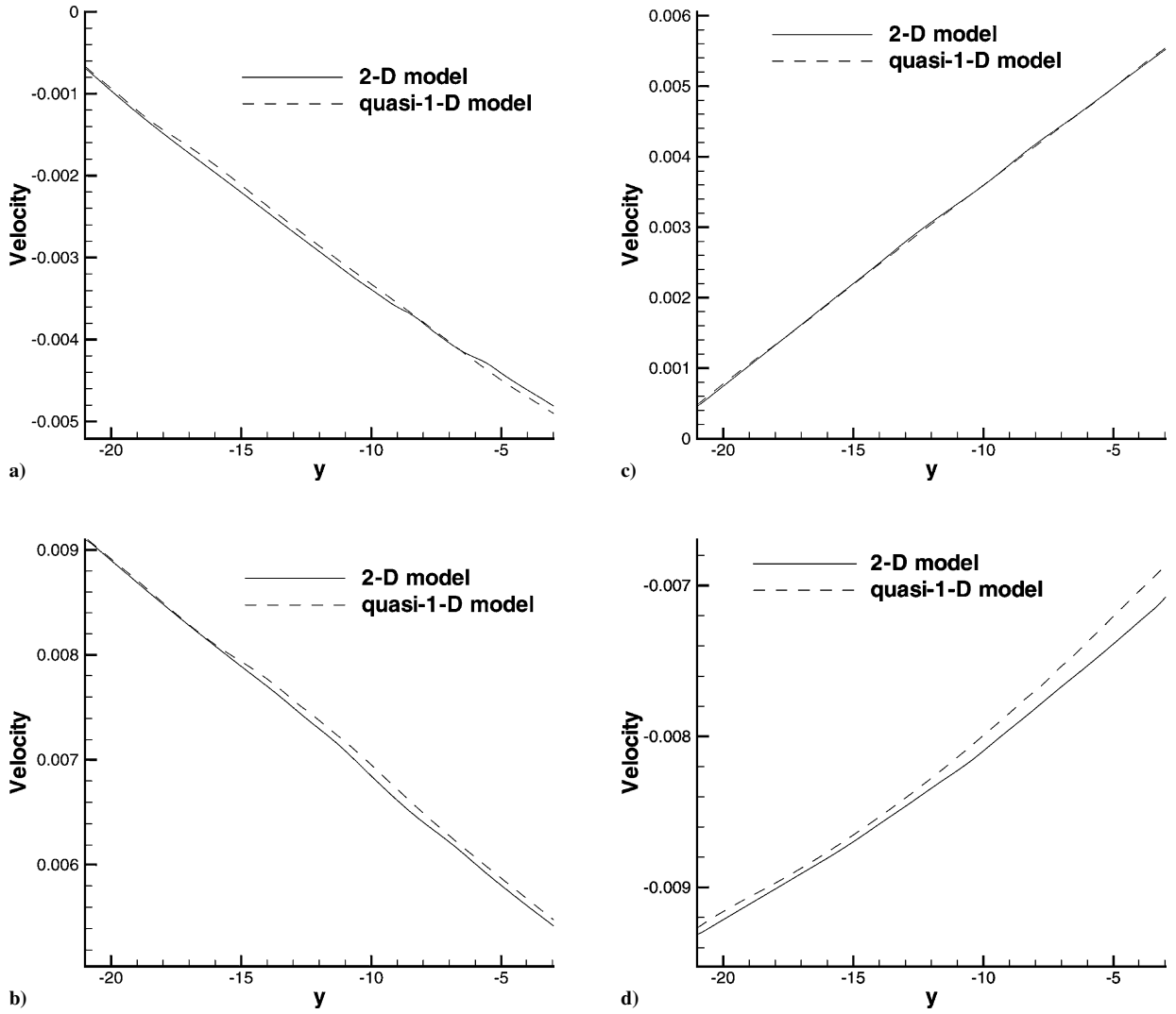

Fig. 15 Instantaneous one-dimensional velocity distributions inside the actuator cavity obtained with quasi-one-dimensional and two-dimensional models for the box actuator at phase angles a) 0, b) $\pi/2$, c) π, and d) $3\pi/2$.

one-dimensionalized full Navier–Stokes solutions is 1–5%. From this comparison, we can conclude that the quasi-one-dimensional model provides the quantitative description of the multidimensional solution inside the actuator cavity in the integral sense.

F. Resonance Characteristics of Synthetic Jet Actuators

It is well known that resonance effects play a crucial role in the improvement of efficiency and performance of synthetic jet actuator devices. From this perspective, it is important to be able to predict and optimize the resonance characteristics of synthetic jet actuators. To demonstrate the ability of the new reduced-order model to simulate the acoustic resonance inherent in synthetic jet actuators, two similar problems are solved. For both problems, a nozzle-type actuator geometry has been chosen to be identical to that used in Sec. V.B. In the first problem, the isolated synthetic jet actuator placed in a quiescent flow is simulated by the fully inviscid quasi-one-dimensional model. The exterior flowfield is also modeled in a quasi-one-dimensional sense by prescription of the appropriate boundary conditions at the quasi-one-dimensional actuator orifice exit. The second problem considers the interaction of the same synthetic jet actuator with a crossflow. The quasi-one-dimensional actuator model is employed to simulate the cavity flow, whereas the exterior crossflow and the small region near the jet exit are modeled with the two-dimensional Navier–Stokes equations. The Reynolds number Re_d is set to be 5×10^2. In both cases, we perform a series of calculations at different frequencies that allow us to quantify the influence of the crossflow and the viscous effects on the actuator resonance characteristics.

Figure 16 shows the peak mass rates at the orifice exit after 10 cycles of diaphragm oscillation, obtained for both cases. Note that each point in each curve corresponds to a separate calculation at a different frequency, and only the peak value of the mass rate obtained in each run is shown in the Fig. 16. The diaphragm amplitude and frequency are chosen such that the peak mass rate at the diaphragm remains unchanged for all of the numerical calculations presented.

Three conclusions can be drawn from this comparison. First, the results presented in Fig. 16 demonstrate that, although the diaphragm pushes the same amount of fluid for all of the frequencies considered, the jet velocity strongly depends on the diaphragm frequency. The main reason for such a behavior is fluid compressibility. In both cases the peak mass rate at the orifice exit exhibits resonance behavior similar to the Helmholtz resonance inherent in cavity flows. If the diaphragm frequency differs from its resonance value $\omega = 0.077$, the peak mass rate drastically decreases. We emphasize that in both cases the resonance mass rate at the orifice exit is more than one order of magnitude larger than its minimum value. In other words, the effectiveness of the synthetic jet actuator can be tremendously improved by optimization of the diaphragm frequency.

Second, the viscous effects considerably decrease the mass rate amplitude at the orifice exit. Because the Reynolds number based

Table 2 Computational time per one nondimensional time unit

Problem	t_{q1d}, s	t_{2D}, s	t_{2D}/t_{q1D}
Nozzle-type actuator with $10d$ neck	129	210	1.63
Box-type actuator with $1d$ neck	172	251	1.46

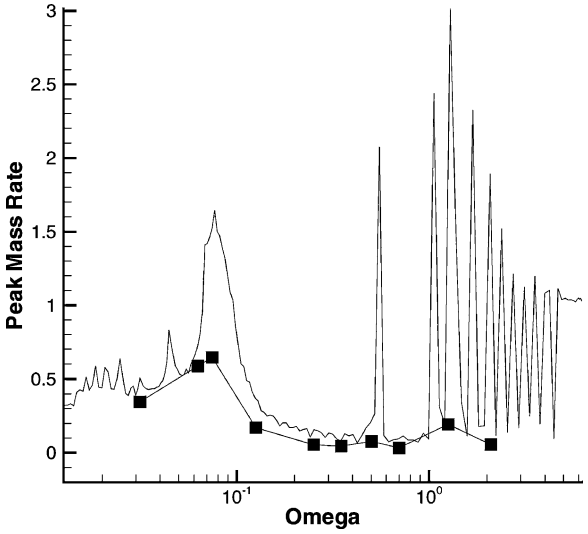

Fig. 16 Effect of the actuator/boundary-layer interaction on the resonance characteristics of the synthetic jet actuator: ——, quasi-one-dimensional actuator in an inviscid quiescent flow and ■, quasi one-dimensional actuator in a viscous crossflow.

on the slot width was set to 5×10^2, the viscosity effects associated with the external boundary-layer/synthetic jet interaction and growth of the viscous layer in the actuator orifice restrict the mass flow through the orifice. As a result, the resonance mass rate amplitude at the orifice exit decreases by a factor of two compared with that obtained with the fully quasi-one-dimensional Euler simulation of the isolated actuator.

Third, the presence of the crossflow and viscosity have almost no effect on the resonance frequency of the synthetic jet actuator. Although the fully developed boundary layer and its separation near the jet exit significantly reduce the mass rate amplitude, the resonances obtained in both cases occur at the same frequency. These results indicate that the inviscid quasi-one-dimensional model can be used to quantitatively predict the resonance frequency of realistic synthetic jet actuators.

G. Efficiency of the Quasi-One-Dimensional Model

Another very important issue that should be addressed is the efficiency of the quasi-one-dimensional model. To evaluate the efficiency of the new reduced-order model, CPU times required for integration of the governing equations over one nondimensional time unit by using both the quasi-one-dimensional model t_{q1D} and the full two-dimensional model t_{2D}, as well as their ratio t_{2D}/t_{q1D}, are compared in Table 2. The test problems presented in Table 2 are those considered in Secs. V.B and V.E. All of the calculations have been performed on a personal computer with a 3-GHz Xeon processor.

As follows from the results presented in Table 2, the new quasi-one-dimensional model is about 1.5 times faster than its two-dimensional counterpart, while providing near full fidelity in the exterior flowfield. Note that the efficiency of the quasi-one-dimensional model increases if a large array of actuators is simulated. Actually, under the assumptions that the region near the orifice exit, which is always simulated with the full Navier–Stokes equations, can be resolved with 1/10 of the two-dimensional computational grid used inside the actuator cavity and that the number of grid points in the exterior flowfield and in the cavity region is approximately the same, the amount of work needed for the simulation of n actuators by the use of the quasi-one-dimensional model can be estimated as follows: $0.1Nn + In + N$, where N is the number of grid points in the two-dimensional cavity region and I is the number of grid points used for the approximation of the quasi-one-dimensional Euler equations. For the two-dimensional model, the amount of work required for simulation of n actuators is $Nn + N$. If $I \ll N$, the quasi-one-dimensional model allows us to simulate n actuators by a factor of $(n+1)/(0.1n+1)$ faster than the full two-dimensional Navier–Stokes simulation of both the exterior and interior flowfields. Note that the actual speed-up t_{2D}/t_{q1D} presented in Table 2 is less than its theoretical limit 1.82 because the entire neck region and the small portion of the actuator cavity (for the box actuator) are simulated with the two-dimensional Navier–Stokes equations. As follows from the analysis presented in Sec. V.D, this region near the orifice exit, where the Navier–Stokes equations are used, can be reduced, thus increasing the efficiency of the quasi-one-dimensional model without sacrificing the accuracy.

VI. Discussion

The broad objective of this study is to present proof of concept for the representation of realistic fluid actuators by reduced-order models based on a quasi-one-dimensional approach. Encouraging results are obtained for all geometries studied. Inevitably, however, some geometries will not be well represented in quasi-one-dimensional form. Likely candidates include three-dimensional actuators that have two or more dominant Helmholtz resonance length scales as opposed to a single dominant scale. A precise statement about the absolute generality of this approach is not currently possible, but this issue is the focus of ongoing work.

Two different geometries are the primary focus of the present study. The first consists of a nozzle-type synthetic jet actuator with a long neck (neck to orifice ratio of 10:1). The second geometry is a box-type symmetric actuator with a short neck (neck to orifice ratio of 1:1). Exact comparisons are made between the quasi-one-dimensional approach and full two-dimensional simulations in both cases, thus allowing a quantitative measure of error. Geometries that did not allow for an exact solution (full two-dimensional simulation) were not considered.

The exact shape and characteristics of realistic actuators continue to evolve with different applications. The shape of actual devices will likely lie between the two extremes presented in this work and will be amenable to the quasi-one-dimensional model. In this respect, it is important to determine how to optimize actuator parameters (size, geometry, and diaphragm frequency) to provide the maximum performance (mass rate at the orifice exit). The best candidate for the solution of this optimization problem is the new reduced-order model because of its efficiency and accuracy.

Ongoing work continues to determine the generality of the quasi-one-dimensional representation for complex devices. It is critical to determine which three-dimensional resonator shapes are not well suited for the quasi-one-dimensional approach. If secondary harmonics are unimportant (moderate accuracy tolerances), perhaps it is possible to model the primary harmonic of a three-dimensional device by an effective quasi-one-dimensional geometry. Another outstanding issue is the fidelity required in the diaphragm region to achieve acceptable levels of global accuracy. Actuator diaphragms can undergo structural resonances that are frequency-related and could interact with the acoustic modes.

VII. Conclusions

The new reduced-order model of a synthetic jet actuator has been proposed and validated. The main idea of the new approach is to use the low-dimensional model of two-dimensional/three-dimensional synthetic jet actuators that is based on the quasi-one-dimensional Euler equations. The oscillating diaphragm is simulated as a quasi-one-dimensional moving boundary. The new reduced-order model possesses the following important characteristics. First, it satisfies the conservation laws. Also, the new reduced-order model is efficient in terms of computational time because only the one-dimensional equations need to be solved. The quasi-one-dimensional model retains important multidimensional features of the realistic actuator governed by the length, area variation, diaphragm deflection, and

frequency and can, therefore, be used for prediction of the synthetic jet dynamics and the actuator resonance characteristics. The proposed reduced-order model is flexible and can be used for a broad class of actuator geometries ranging from smooth nozzle-type to nonsmooth box-type profiles. Furthermore, the fluid/structure interaction can be included in the new quasi-one-dimensional actuator model by the addition of the terms associated with the structural stiffness of the actuator membrane. Because the actuator is simulated in a quasi-one-dimensional sense, the new model does not take into account the multidimensional effects associated with the vortex generation, boundary layer, and the boundary-layer separation inside the actuator cavity. However, quantitative comparison of the quasi-one-dimensional and full two-dimensional models shows that if the Reynolds number based on the actuator slot width is larger than 5×10^2 and the interface between the quasi-one-dimensional Euler equations and the two-dimensional Navier–Stokes equations is located more than $2d$ away from the jet exit, then the new reduced-order model provides high accuracy in the exterior flowfield. Another important conclusion is that only the multidimensional effects near the jet exit are essential: These should be simulated by the use of the full Navier–Stokes equations, whereas the cavity flow can be accurately predicted by the quasi-one-dimensional Euler equations. One of the main advantages of the new reduced-order model is its ability to predict the acoustic resonance inherent in synthetic jet actuators. As follows from the numerical study of the actuator resonance characteristics, the synthetic jet mass rate at the orifice exit can be increased by more than one order of magnitude by moving the diaphragm at the acoustic resonance frequency. The developed reduced-order model opens new avenues for the detailed study of synthetic jet actuators and optimization of their performance, which is not feasible with the existing methodologies based on either the zero-dimensional or three-dimensional model.

References

[1]Smith, B. L., and Glezer, A., "Vectoring and Small-Scale Motions Effected in Free Shear Flows Using Synthetic Jet Actuators," AIAA Paper 97-0213, Jan. 1997.

[2]Kral, L. D., Donovan, J. F., Cain, A. B., and Cary, A. W., "Numerical Simulation of Synthetic Jet Actuators," AIAA Paper 97-1824, June 1997.

[3]Donovan, J. F., Kral, L. D., and Cary, A. W., "Active Flow Control Applied to an Airfoil," AIAA Paper 98-0210, Jan. 1998.

[4]Hassan, A. W., and JanakiRam, R. D., "Effects of Zero-Mass Synthetic Jets on the Aerodynamics of the NACA-0012 Airfoil," *Journal of the American Helicopter Society*, Vol. 43, Oct. 1998, pp. 303–311.

[5]Carlson, H. A., and Lumley, J. L., "Flow over an Obstacle Emerging from the Wall of a Channel," *AIAA Journal*, Vol. 34, No. 5, 1996, pp. 924–931.

[6]Hoffmann, L. M., and Herbert, T., "Disturbances Produced by the Motion of an Actuator," *Physics of Fluids*, Vol. 9, No. 12, 1997, pp. 3727–3732.

[7]Lin, H., and Chieng, C. C., "Computations of Compressible Synthetic Jet Flows Using Multigrid/Dual Time Stepping Algorithm," AIAA Paper 99-3114, June–July 1999.

[8]Carpenter, P. W., Lockerby, D. A., and Davies, C., "Numerical Simulation of the Interaction of Microactuators and Boundary Layers," *AIAA Journal*, Vol. 40, No. 1, 2002, pp. 67–73.

[9]Rathnasingham, R., and Breuer, K. S., "Characteristics of Resonant Actuators for Flow Control," AIAA Paper 96-0311, Jan. 1996.

[10]Gallas, Q., Mathew, J., Kaysap, A., Holman, R., Nishida, T., Carrol, B., Sheplak, M., and Cattafesta, L., "Lumped Element Modeling of Piezoelectric-Driven Synthetic Jet Actuators," *AIAA Journal*, Vol. 41, No. 2, 2003, pp. 240–247.

[11]Rizzetta, D. P., Visbal, M. P., and Stanek, M. J., "Numerical Investigation of Synthetic Jet Flowfields," *AIAA Journal*, Vol. 37, No. 8, 1999, pp. 919–927.

[12]Joslin, R. D., Lachowicz, J. T., and Yao, C. S., "DNS of Flow Induced by a Multi-Flow Actuator," *Proceedings of the ASME Fluids Engineering Conference, Forum on Control of Transitional and Turbulent Flows*, American Society of Mechanical Engineers, Fairfield, NJ, 1998, Paper FEDSM 98-5302.

[13]Mittal, R., Ramunggoon, P., and Udaykumar, H. S., "Interaction of a Synthetic Jet with a Flat Plate Boundary Layer," AIAA Paper 2001-2773, June 2001.

[14]Lee, C. Y., and Goldstein, D. B., "Two-Dimensional Synthetic Jet Simulation," *AIAA Journal*, Vol. 40, No. 3, 2002, pp. 510–516.

[15]Seifert, A., Bachar, T., Koss, D., Shepshelovich, M., and Wyganski, I., "Oscillatory Blowing: A Toll to Delay Boundary-Layer Separation," *AIAA Journal*, Vol. 31, No. 11, 1993, pp. 2052–2060.

[16]Seifert, A., Darabi, A., and Wyganski, I., "Delay of Airfoil Stall by Periodic Excitation," *Journal of Aircraft*, Vol. 33, No. 4, 1996, pp. 691–698.

[17]Kennedy, C. A., Carpenter, M. H., and Lewis, R., "Low-Storage, Explicit Runge–Kutta Schemes for the Compressible Navier–Stokes Equations," *Applied Numerical Mathematics*, Vol. 35, No. 3, 2000, pp. 177–219.

S. Aggarwal
Associate Editor